HE & VHE emissions from rapidly rotating black holes

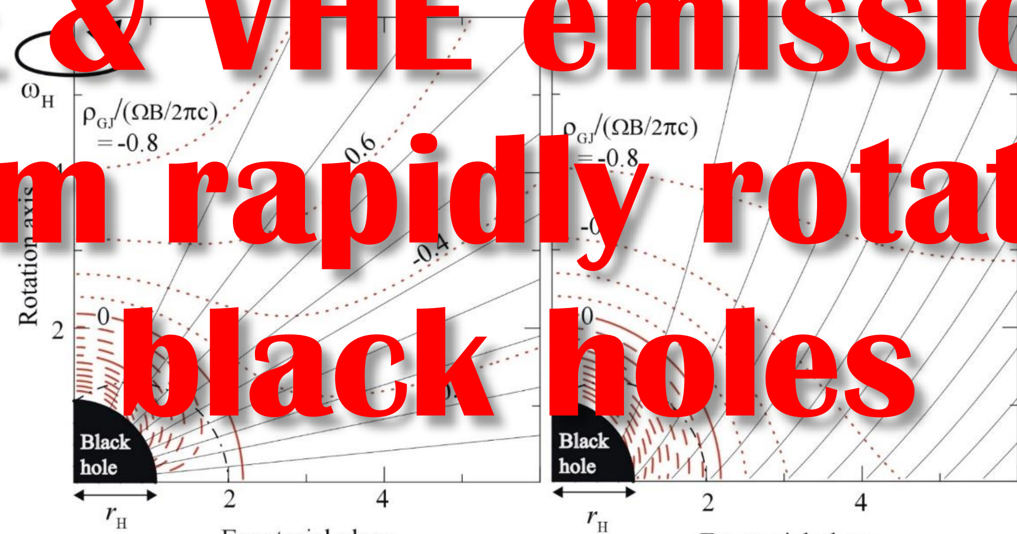

Side view of BH magnetosphere

Kouichi HIROTANI

ASIAA, Taiwan,

ICRR, U. of Tokyo

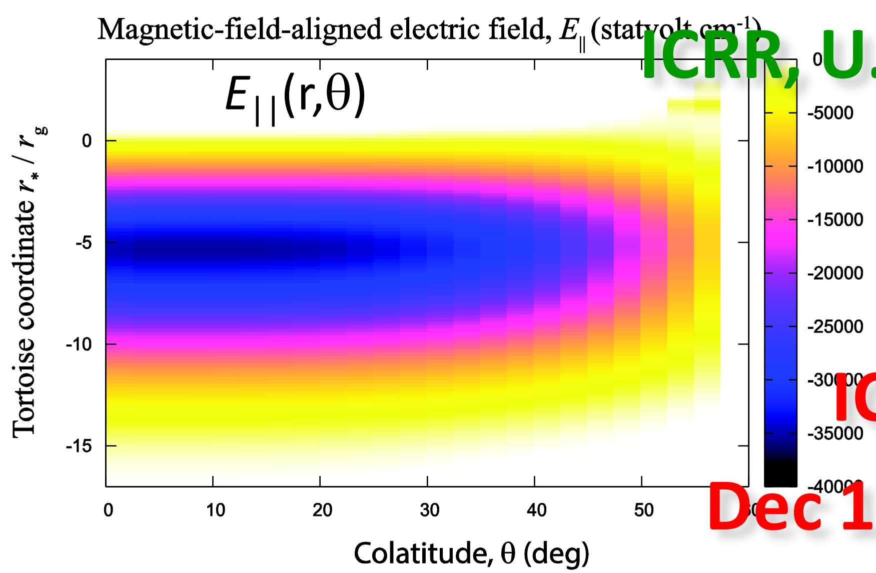

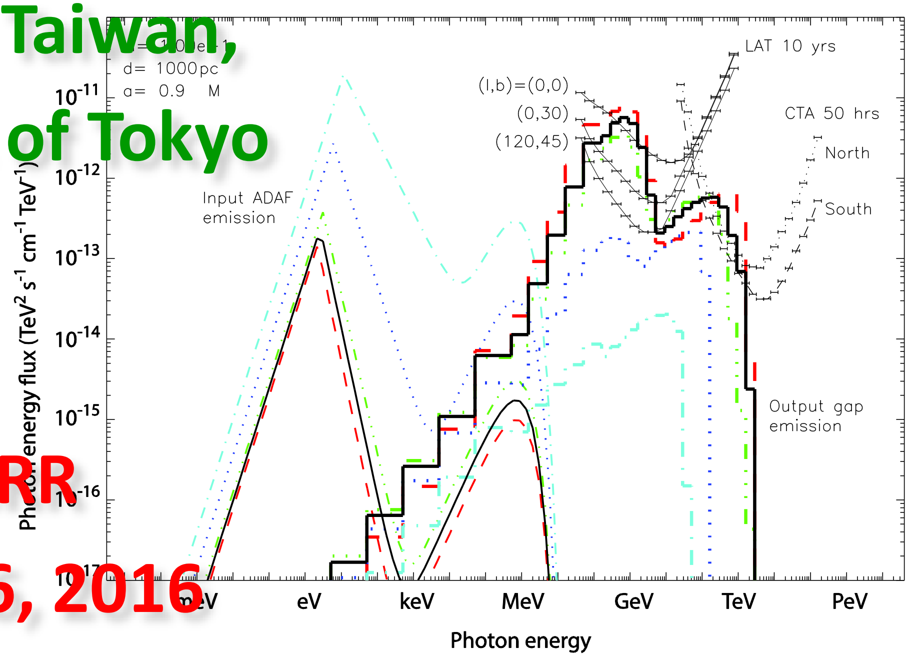

ICRR

Dec 16, 2016

§ 1 Introduction

So far, 77 X-ray binary BHs and BHCs have found in MW & LMC.

BlackCAT (Corral-Santana + ’16, AA 587, A61)
WATCHDOG (Tetarenko + ’16, ApJS 222, 15)

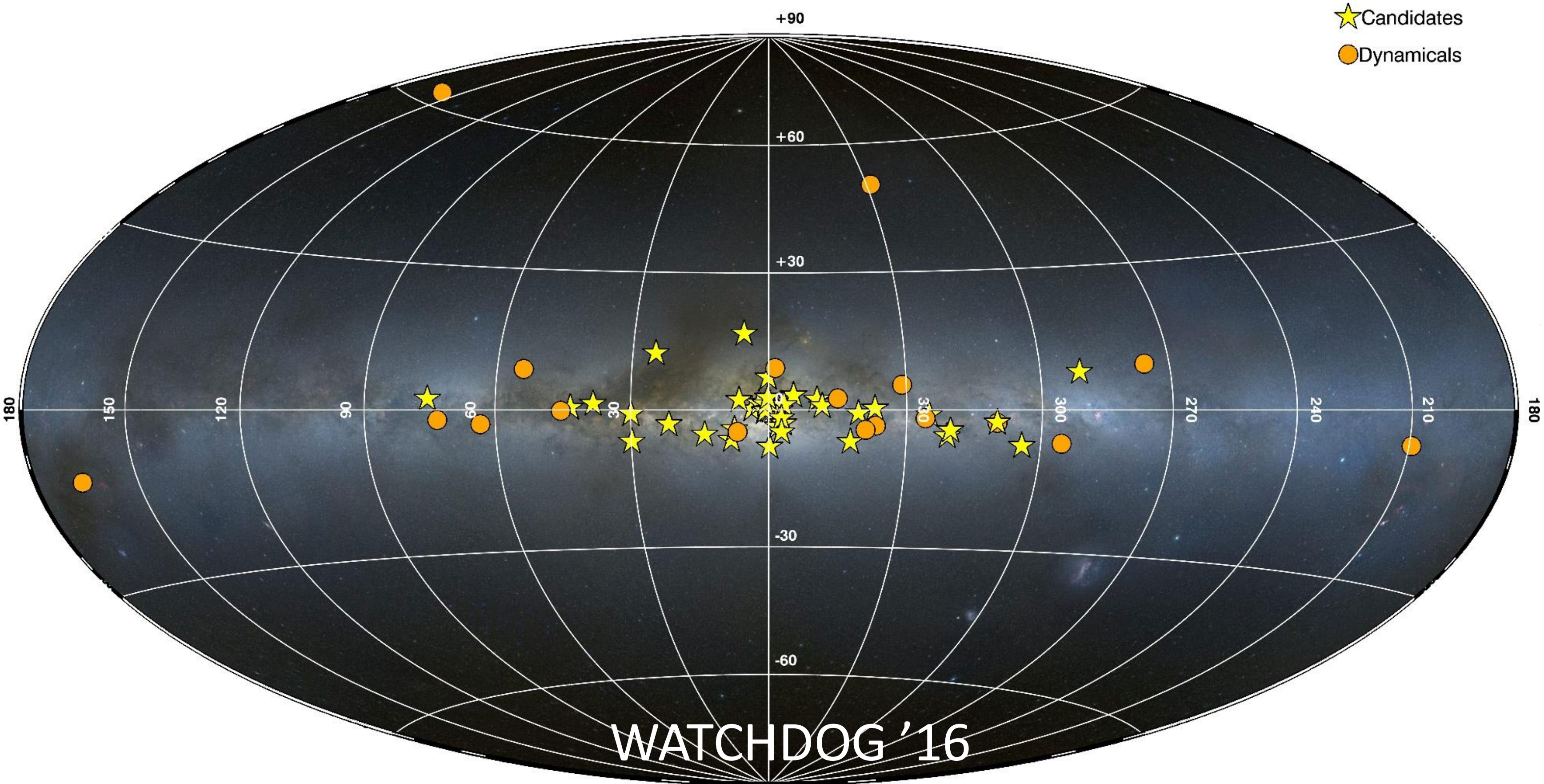

§ 1 Introduction

So far, 77 X-ray binary BHs and BHCs have found in MW & LMC.

BlackCAT (Corral-Santana + ’16, AA 587, A61)
WATCHDOG (Tetarenko + ’16, ApJS 222, 15)

In these BH X-ray binaries, material transfers from a companion star onto the BH primary.

HMXBs 6 are fed by wind, 1 by Roche-lobe overflow
Companion: O-B stars ($M>10M_\odot$)

LMXBs 45 are fed by Roche-lobe overflow.
Companion: K-M ($M<M_\odot$) or B-F ($M \sim M_\odot$)

(Companion nature of other 26 BHXBs are unknown.)

§ 1 Introduction

The mass accretion rate $\dot{M}$ near the compact object determines their emission properties.

6 BH-HMXBs and 4 BH-LMXBs have $\dot{M} > 10^{-8}\ M_{\odot}\mathrm{yr}^{-1}$, showing persistent X-ray emission with $L_X \sim L_{\mathrm{Edd}}$.

Tanaka & Shibazaki 1996, ARA&A 34, 607

47 BH-LMXBs have much lower long-term accretion rate, $\dot{M} < 10^{-9}\ M_{\odot}\mathrm{yr}^{-1}$, showing transient X-ray emission: Sporadic outbursts after long-time quiescence.

Tanaka & Lewin 1995, in *X-ray binaries*, p. 126

Outburst recurrence period ranges $10^{0\text{-}2}$ yrs.

WATCHDOT, BlackCAT

§ 1 Introduction

For transient BH binaries, HE & VHE emissions are expected in the shock-in-jet model.

Marscher & Gear 1985, ApJ 298, 114

HE/VHE flux increases w/ increasing $\dot{M}$.

However, HE/VHE emissions are also predicted to be emitted in the BH-gap model from transient BHBs.

KH & Pu 2016, ApJ 818, 50; KH + 2016, ApJ in press

HE/VHE flux increases w/ decreasing $\dot{M}$.

Today, we will focus on the BH-gap model and discuss its theoretical predictions.

§ 1 Introduction

A quick review of the BH gap model:

Beskin et al. (1992, Sov. Astron., 36, 642) first proposed the BH gap model, extending the pulsar gap model (Cheng + 1986, ApJ 300, 500).

K.H. & Okamoto (1998, ApJ 497, 563) then showed that sufficient plasmas can be supplied via γ-γ pair production around super-massive BHs.

However, predicted γ-ray fluxes were undetectable, because they assumed high accretion rates (as in QSOs), which leads to a very thin gap width ($w \ll r_g$) along **B** lines, where $r_g = GMc^{-2}$.

§ 1 Introduction

A quick review of the BH gap model:

Thus, Neronov & Aharonian (2007, ApJ 671, 85) and Levinson & Rieger (2011, ApJ 730, 123) revisited the BH gap model, adopting much thicker gap width ($w \sim r_g$) and examined M87* and Sgr A*.

Then Broderick & Tchekhovskoy (2015, ApJ 809, 97) showed that two-stream instability does not grow in BH gaps.

Subsequently, KH & Pu (2016, ApJ 818, 50) showed that SMBHs can emit detectable gap emission in VHE if located within a few tens of Mpc.

§ 1 Introduction

Due to frame dragging, the GR Goldreich-Julian charge density, ρ_{GJ}, vanishes near the $\Omega=\omega$ surface (and hence in the direct vicinity of the horizon).

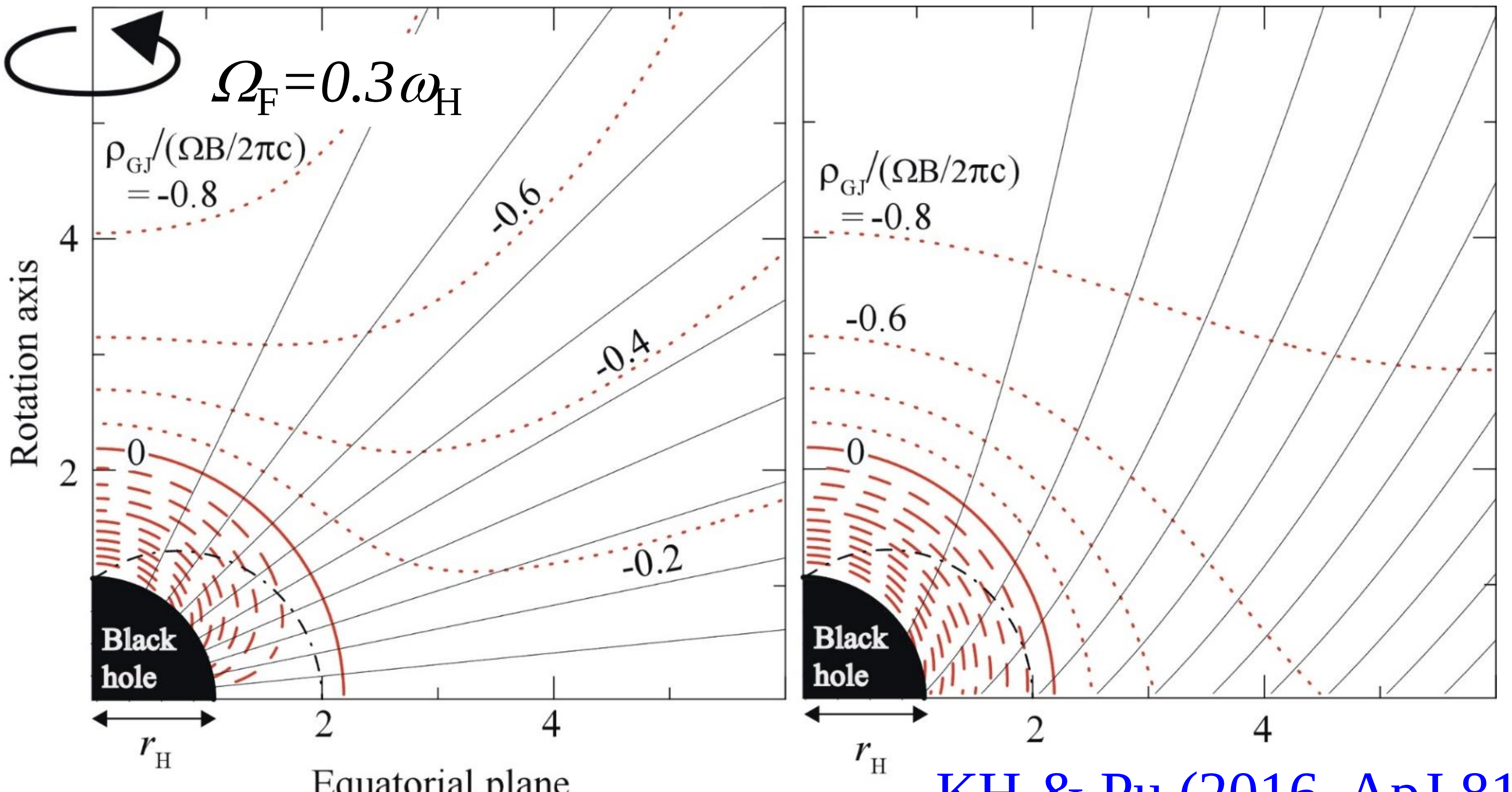

KH & Pu (2016, ApJ 818, 50)

§ 1 Introduction

Around this null surface (ρ_{GJ} =0), a stationary vacuum gap (i.e., $e^{\pm}$ accelerator) arises.

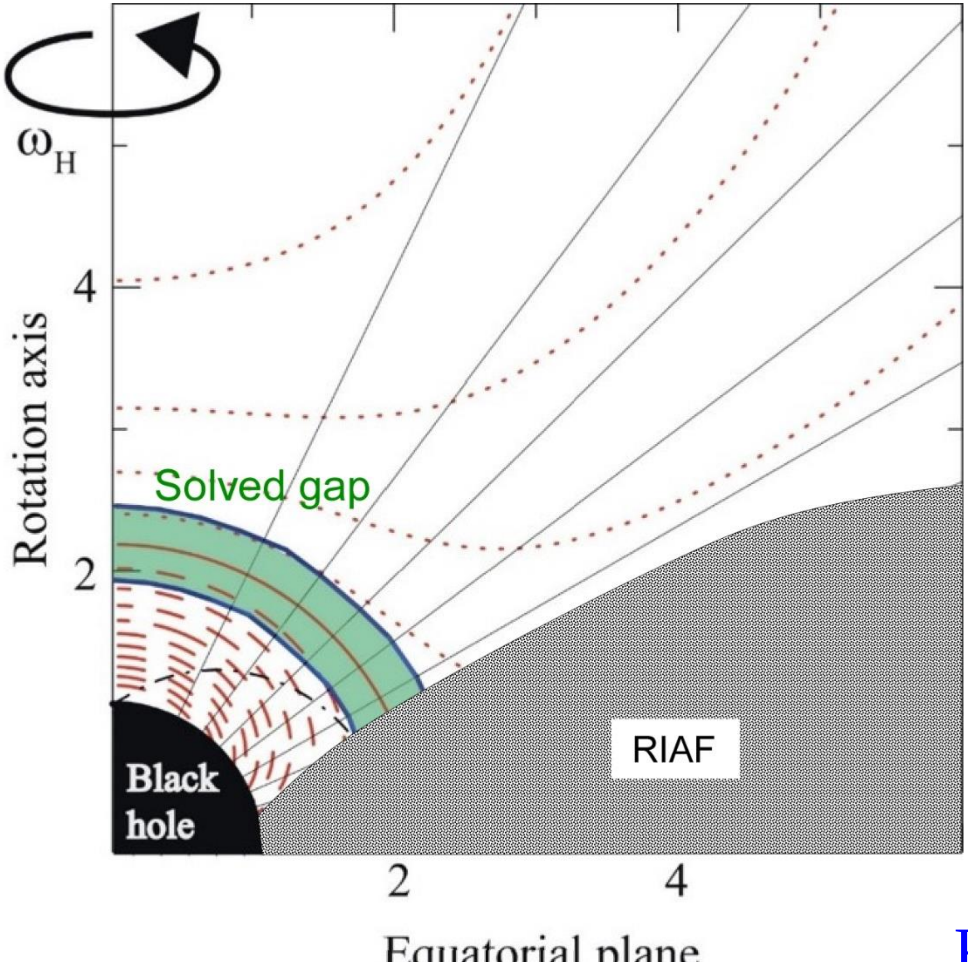

Fig. Side view of a BH gap. Copious HE/VHE emissions are emitted from the green shaded region.

KH & Pu (2016, ApJ 818, 50)

§ 2 Method

Since the null surface appears near the horizon, the same method as the pulsar outer-gap model can be applied to the BH-gap model.

$e^{\pm}$'s are accelerated by $E_{\|}$

↓

Relativistic e^+/e^- emit γ-rays via synchro-curvature, and IC processes

↓

γ-rays collide with soft photons/B to materialize as pairs in the accelerator

§ 2 Method: Basic equations

Beskin + (1992)

Poisson eq. From $\nabla \bullet E = 4\pi\rho$, we obtain

$$\nabla \bullet E_{\parallel} = 4\pi(\rho - \rho_{\mathrm{GJ}}),$$

where

α: redshift factor

$$\rho_{\mathrm{GJ}} \equiv -\frac{1}{4\pi}\nabla \bullet \left(\frac{\Omega_{\mathrm{F}} - \omega}{2\pi\alpha c} \nabla \Psi \right),$$

$\alpha \to 0$ @ horizon

$\alpha \to 1$ @ infinity

$$\mathbf{B}_p = -\frac{e_\phi \times \nabla \Psi}{2\pi\varpi},$$

ϖ : distance from rotation axis.

If $\rho \neq \rho_{\mathrm{GJ}}$ in any region, $E_{\parallel} \neq 0$ arises around it.

$\rho_{\mathrm{GJ}} = 0$ near $\omega = \Omega_{\mathrm{F}}$. Thus, pulsar-like 'null charge surface' appears near the horizon. A vacuum gap can arise there.

§ 2 Method: Basic equations

KH+ ('06, ApJ in press)

$E_\parallel$ is solved from the **Poisson eq.**

Near the horizon ($\Delta \equiv r^2 - 2Mr + a^2 \ll M^2$), it becomes

$$-\left(\frac{r^2+a^2}{\Delta}\right)^2 \frac{\partial^2 \Phi}{\partial r_*^2} + \frac{2(r-r_g)(r^2+a^2)}{\Delta^2} \frac{\partial \Phi}{\partial r_*}$$

$$-\frac{\Sigma}{\Delta \sin\theta} \frac{\partial}{\partial \theta}\left(\frac{\sin\theta}{\Sigma} \frac{\partial \Phi}{\partial \theta}\right) = \left(\frac{\Sigma}{r^2+a^2}\right)^2 (n_+ - n_- - n_{\mathrm{GJ}})$$

where $E_\parallel \equiv -(\mathbf{B} \bullet \nabla)\Phi / B$ and $\Sigma \equiv r^2 + a^2 \cos^2\theta$.

The tortoise coordinate r_* is related to the polar r by

$$\frac{dr_*}{dr} = \frac{r^2+a^2}{\Delta}$$

§ 2 Method: Basic equations

KH+ ('06, ApJ in press)

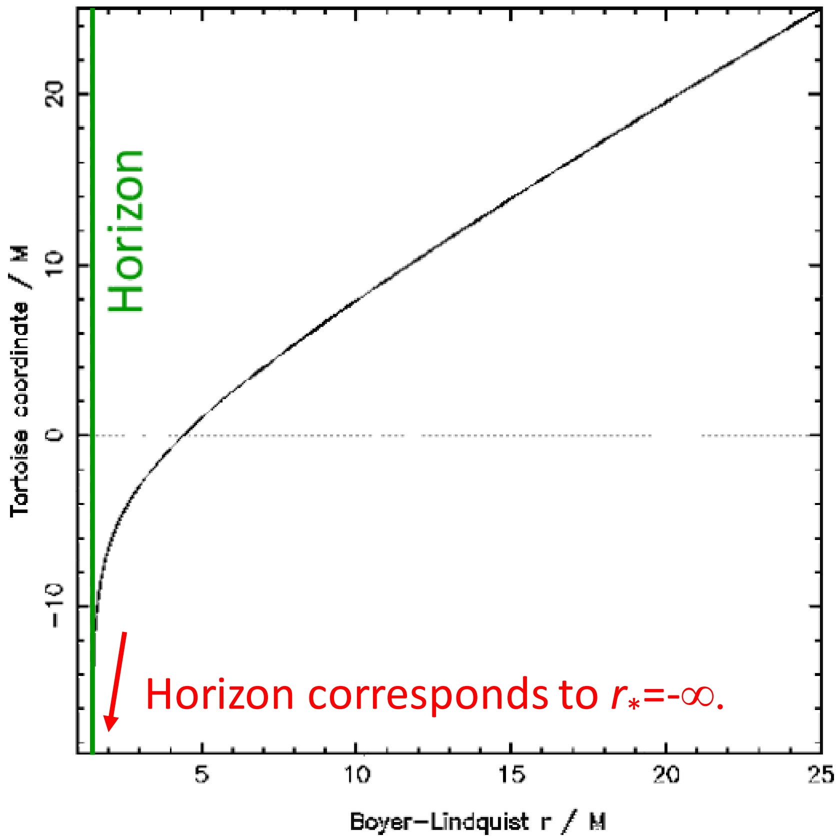

Tortoise coordinate vs. Boyer-Lindquist *r* coordinate

The tortoise coordinate r_* is related to the polar r by

$$\frac{dr_*}{dr} = \frac{r^2 + a^2}{\Delta}$$

§ 2 Method: Basic eqs.

Poisson eq.:

$$-\left(\frac{r^2+a^2}{\Delta}\right)^2\frac{\partial^2\Phi}{\partial {r_*}^2}+\frac{2(r-r_g)(r^2+a^2)}{\Delta^2}\frac{\partial\Phi}{\partial r_*}$$

$$-\frac{\Sigma}{\Delta\sin\theta}\frac{\partial}{\partial\theta}\left(\frac{\sin\theta}{\Sigma}\frac{\partial\Phi}{\partial\theta}\right)=\left(\frac{\Sigma}{r^2+a^2}\right)^2(n_+-n_--n_{\mathrm{GJ}})$$

Instead of solving the $e^{\pm}$ **Boltzmann eqs**., we assume that the Lorentz factors are saturated by curvature- or IC-drag forces and put $\gamma=\min(\gamma_{\mathrm{curv}},\gamma_{\mathrm{ICS}})$. Solve n_+ & n_- from the pair production, which is solved from the γ-ray specific intensity, I_ν at each point.

Radiative transfer eq.: $$\frac{dI_\nu}{dl}=-\alpha_\nu I_\nu+j_\nu$$

§ 3 Results: the case of stellar-mass BHs

Consider a stellar-mass BH, $M = 10M_{\odot}$, assuming $B = B_{eq}$.

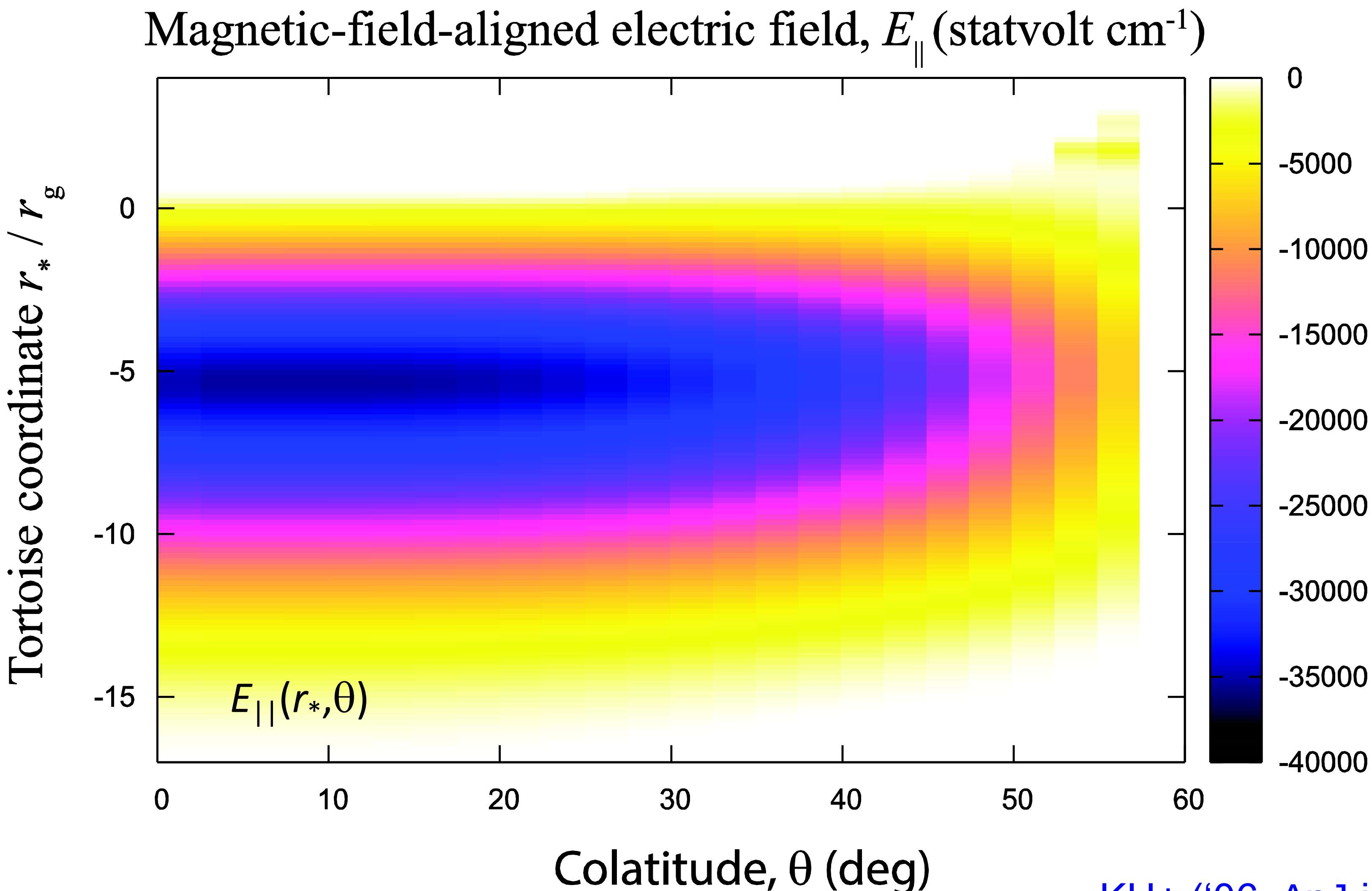

KH+ (‘06, ApJ in press)

§ 3 Results: stellar-mass BHs

$M=10M_{\odot}$, $B=B_{eq}$.

Slice $E_{\|}(r_*,\theta)$ at six θ's.

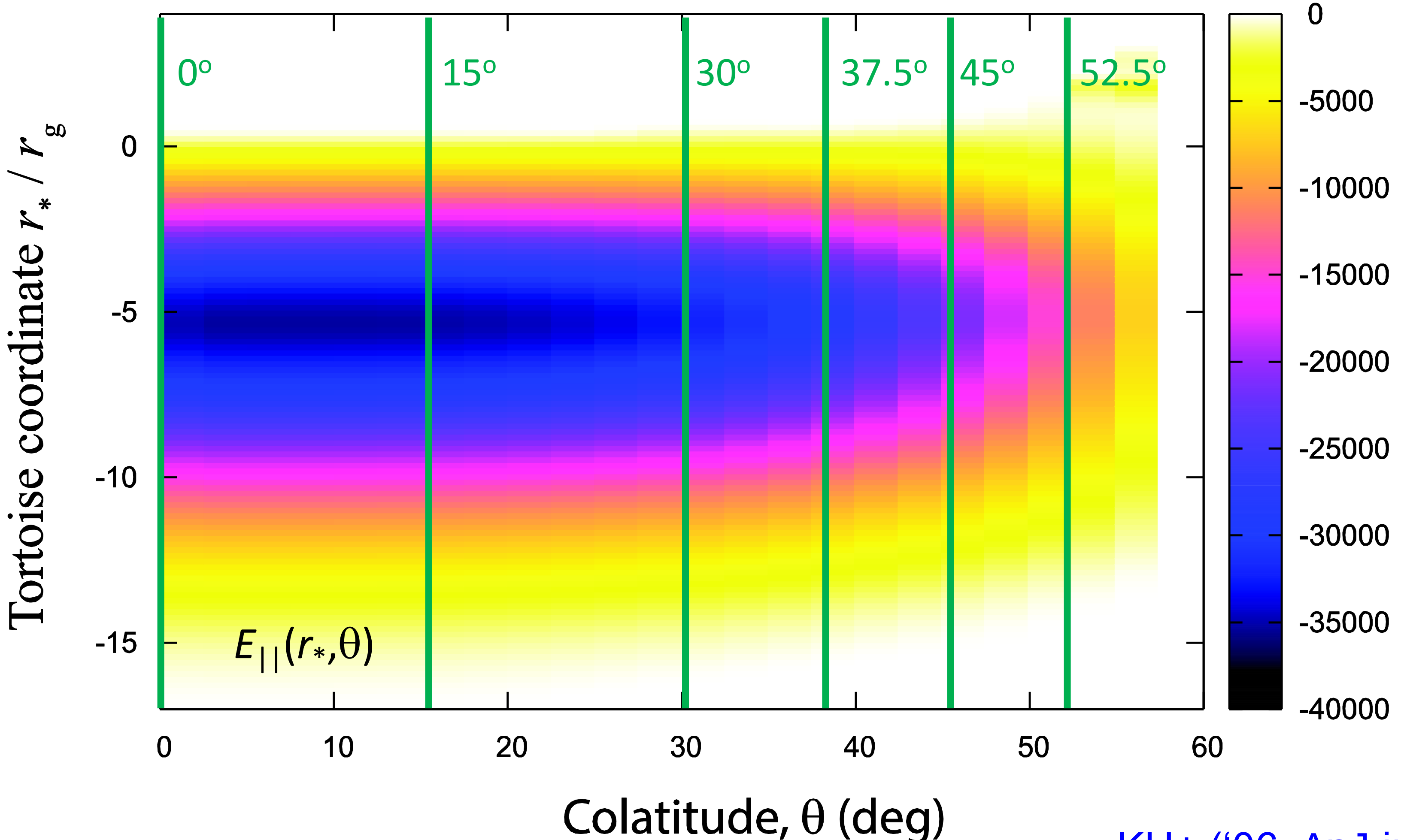

KH+ ('06, ApJ in press)

§ 3 Results: stellar-mass BHs

$M=10M_\odot$, $B=B_{eq}$ Acceleration electric field along **B**

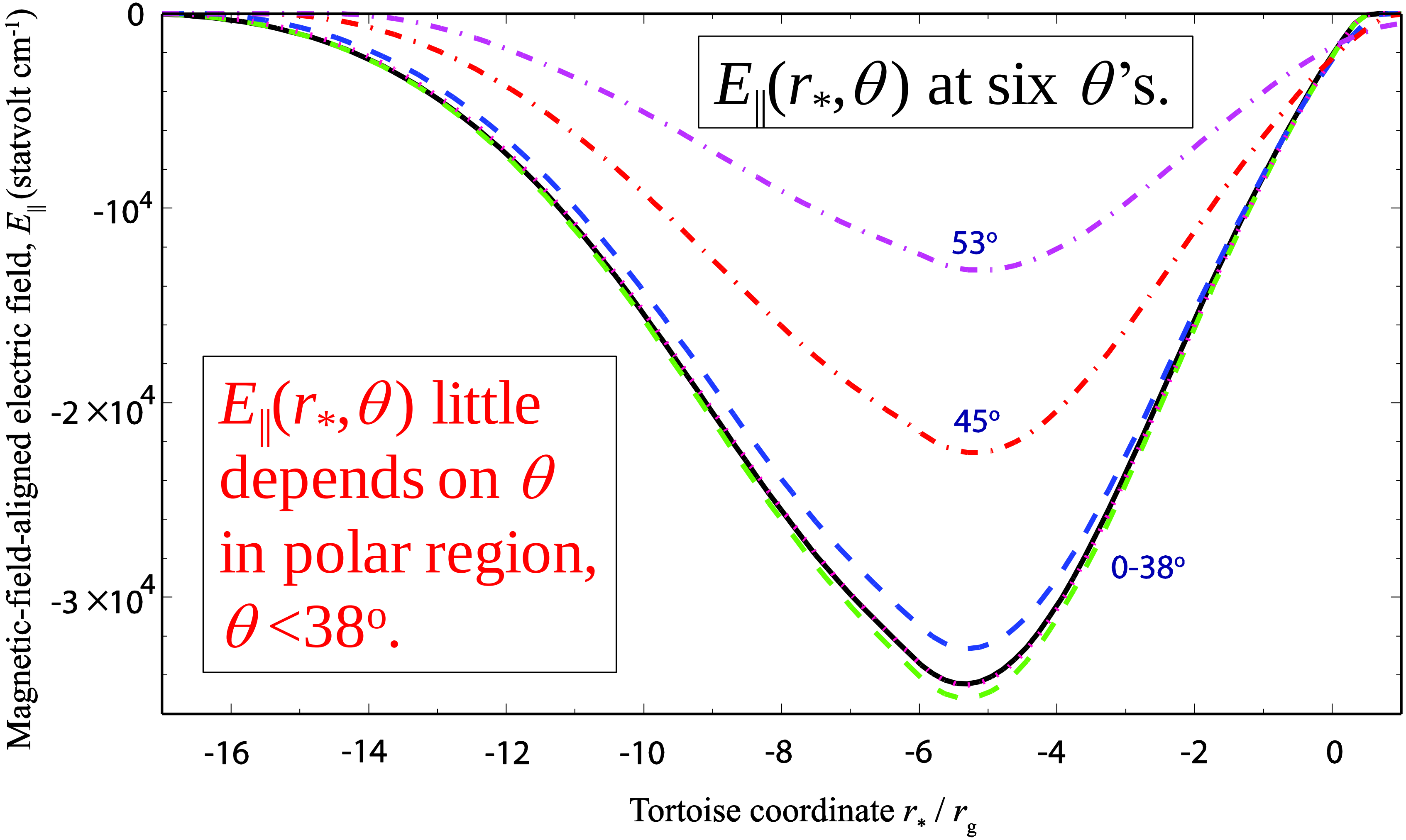

KH+ ('06, ApJ in press)

§ 3 Results: stellar-mass BHs

$M=10M_{\odot}$, $B=B_{eq}$

γ-ray spectra

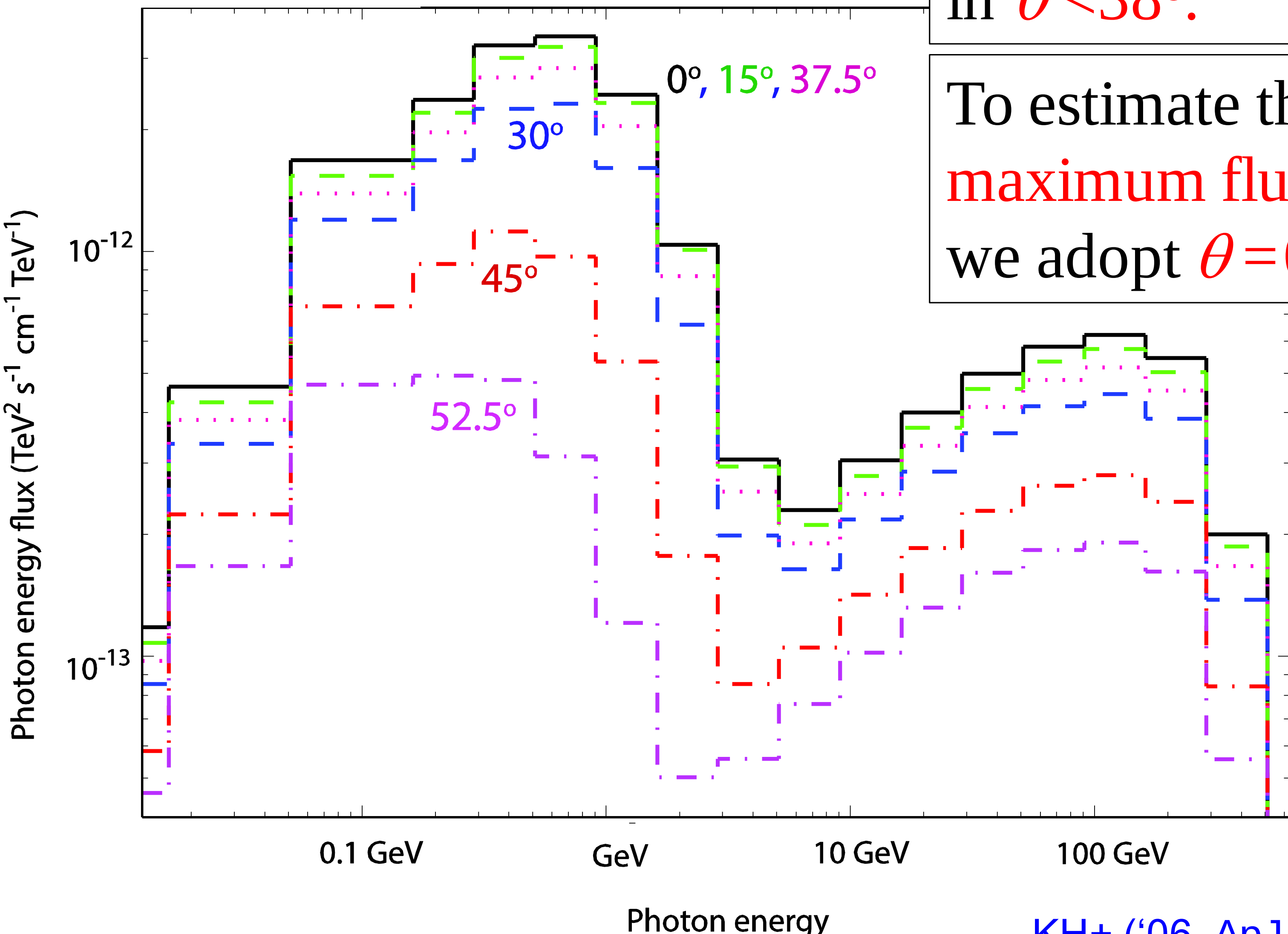

SED little changes in $\theta < 38^{o}$.

To estimate the maximum flux, we adopt $\theta = 0^{o}$.

KH+ ('06, ApJ in press)

§ 3 Results: stellar-mass BHs

$M = 10 M_{\odot}$, $B = B_{eq}$; Lepton densities per **B** flux @ $\theta = 0^{o}$

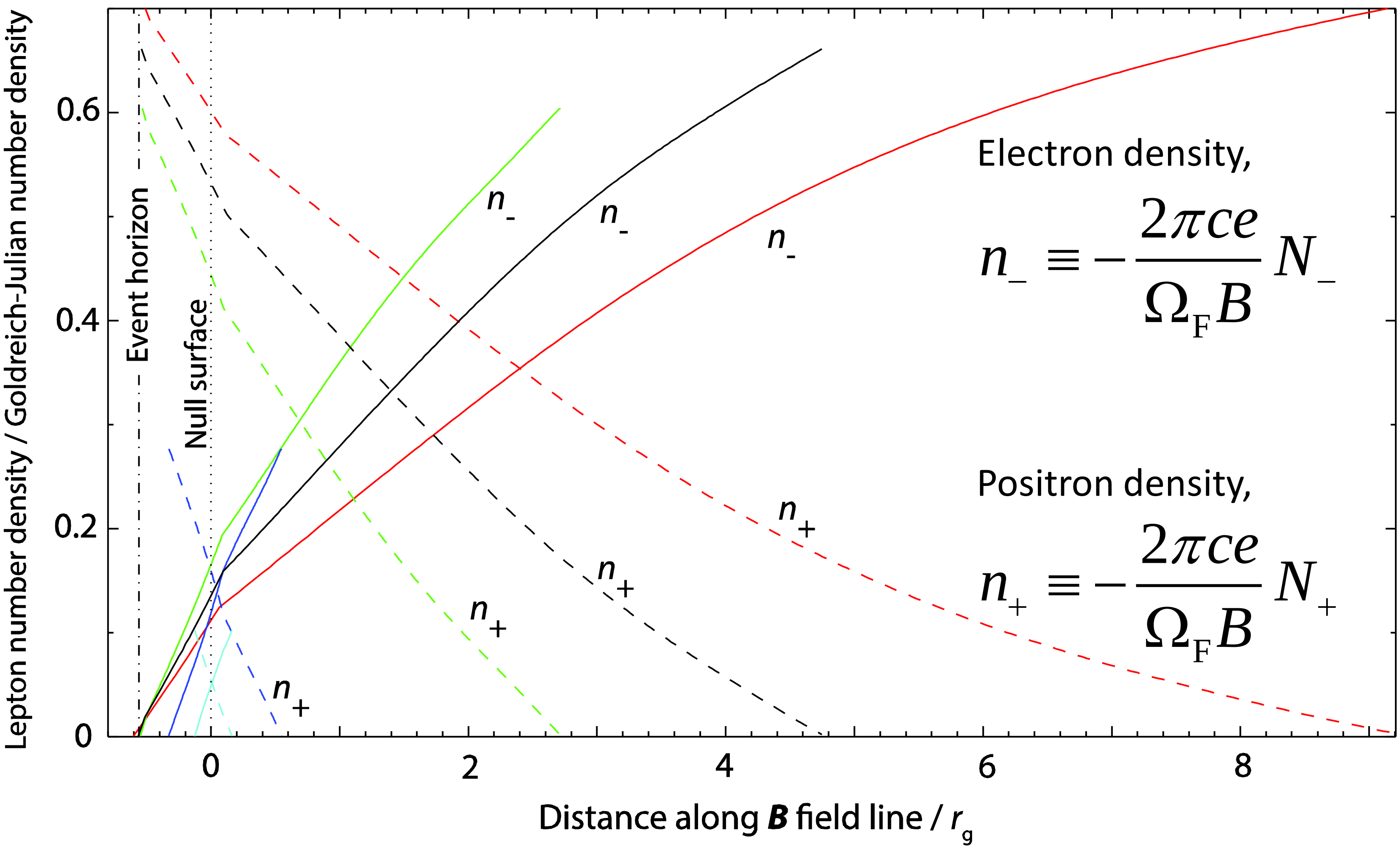

KH+ ('06, ApJ in press)

§ 3 Results: stellar-mass BHs

$M=10M_{\odot}$, $B=B_{eq}$; $E_{\|}(r-r_0,\theta)$ @ $\theta=0^o$

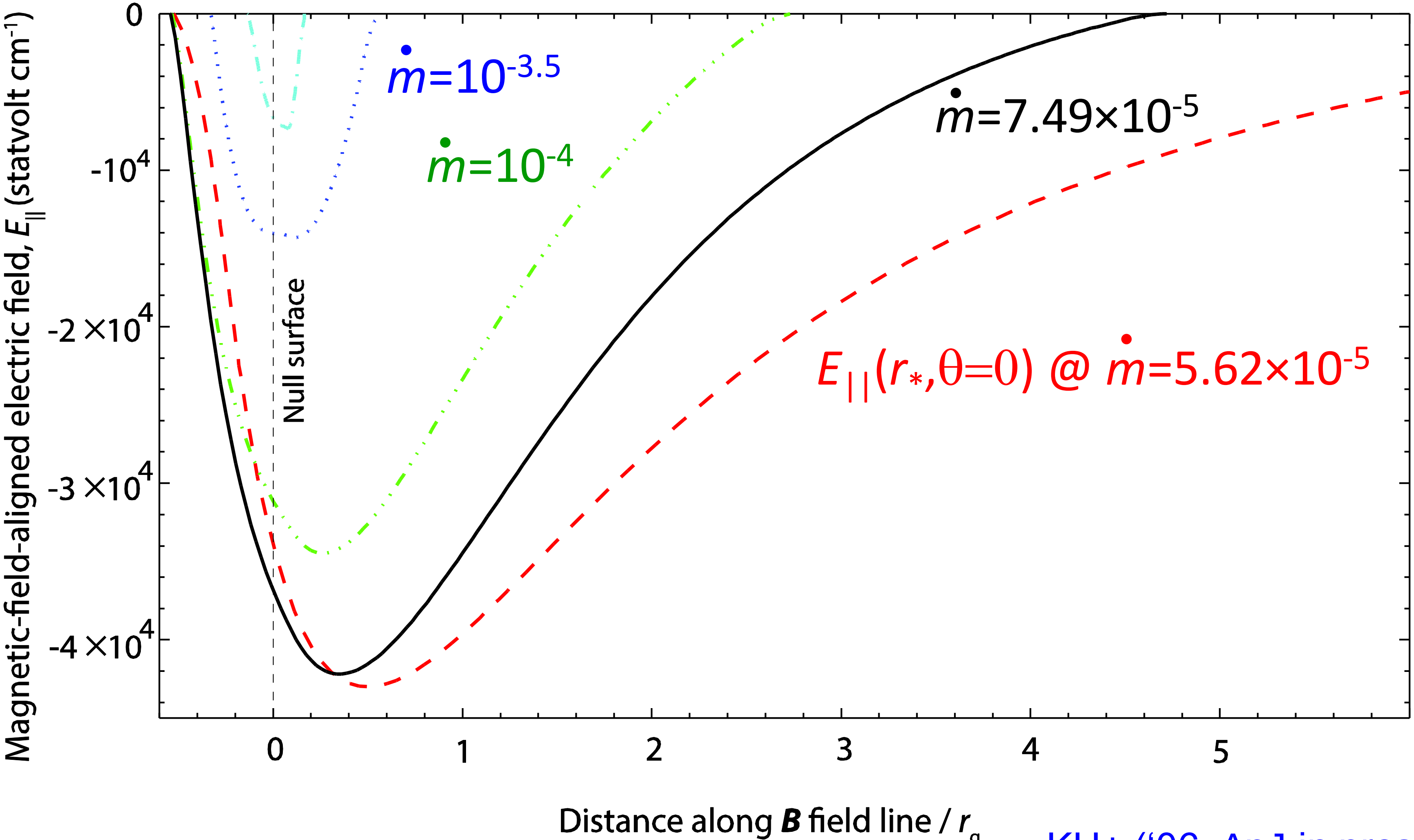

KH+ ('06, ApJ in press)

§ 3 Results: stellar-mass BHs

$M=10M_{\odot}$, $B=B_{eq}$; outer & inner boundaries @ $\theta=0^{o}$

Gap width increases with decreasing accretion rate.

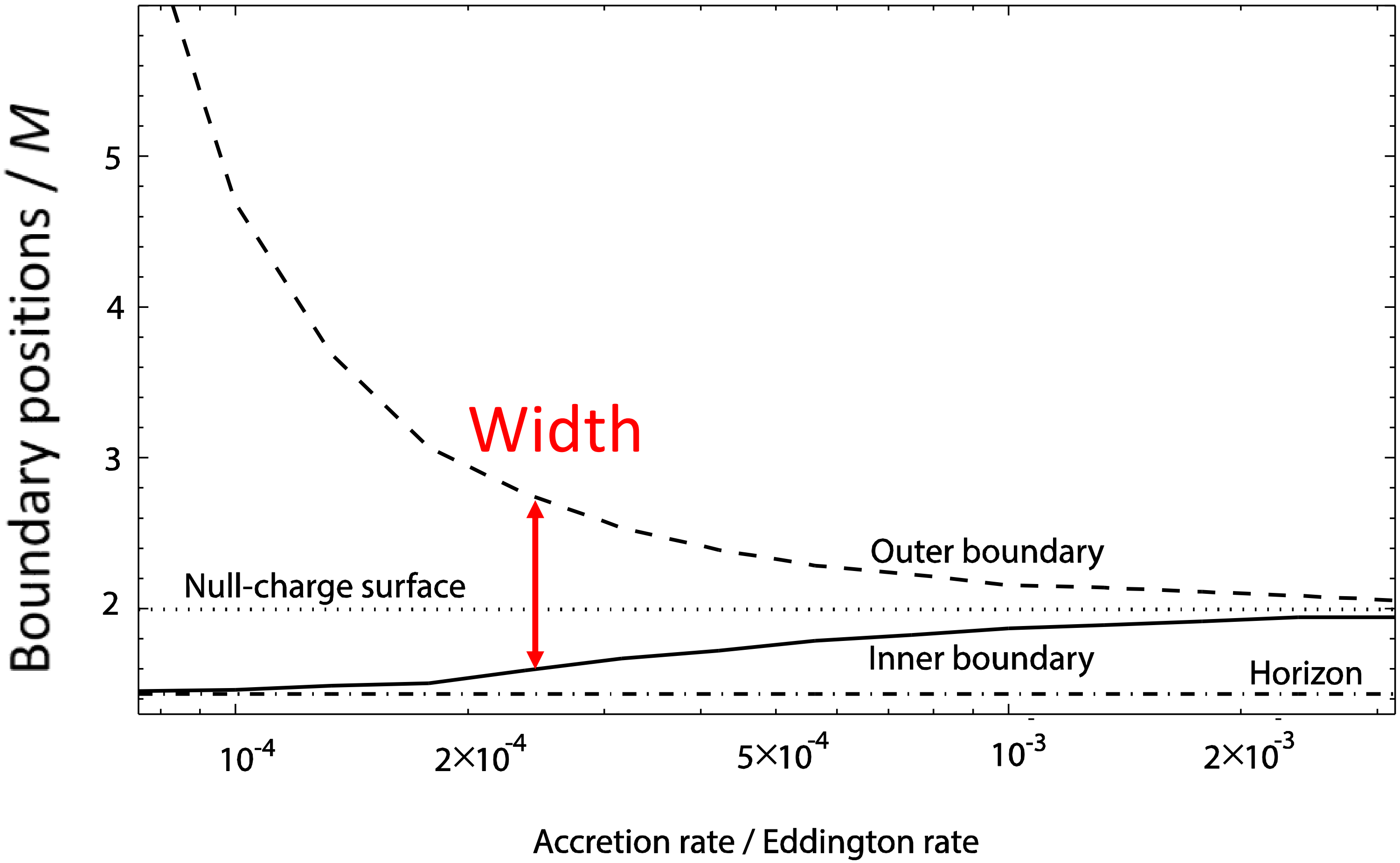

KH+ ('06, ApJ in press)

§ 3 Results: stellar-mass BHs

$M=10M_\odot$, $B=B_{eq}$; SED vs. current density, j ($\theta=0$).

$j\sim0.7$ optimizes HE & VHE fluxes.

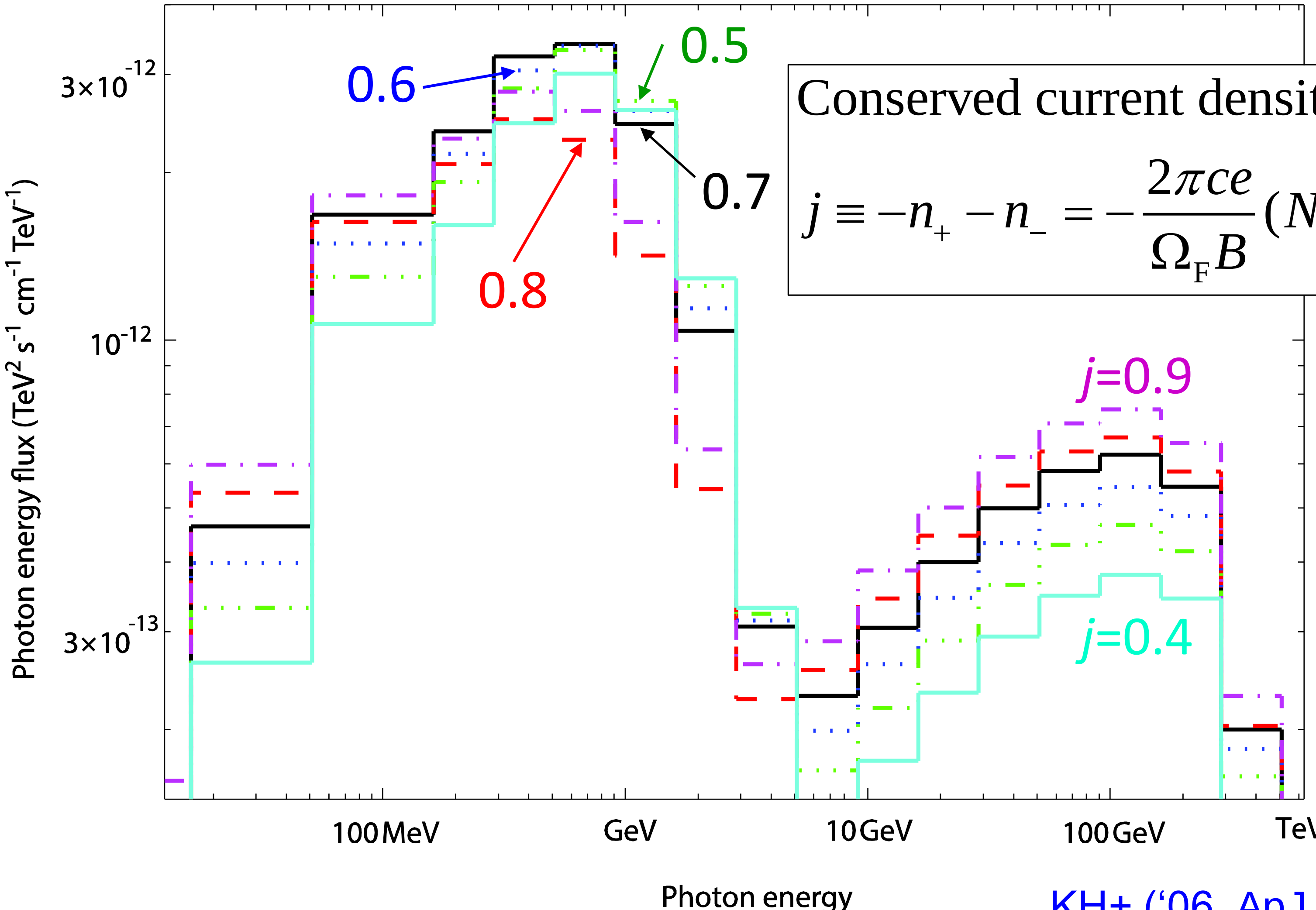

Conserved current density,

$$j \equiv -n_+ - n_- = -\frac{2\pi ce}{\Omega_F B}(N_+ + N_-)$$

KH+ ('06, ApJ in press)

§ 3 Results: stellar-mass BHs

$M=10M_\odot$, $B=B_{eq}$; SEDs @ five discrete $\dot{m}$ ($\theta=0^o$)

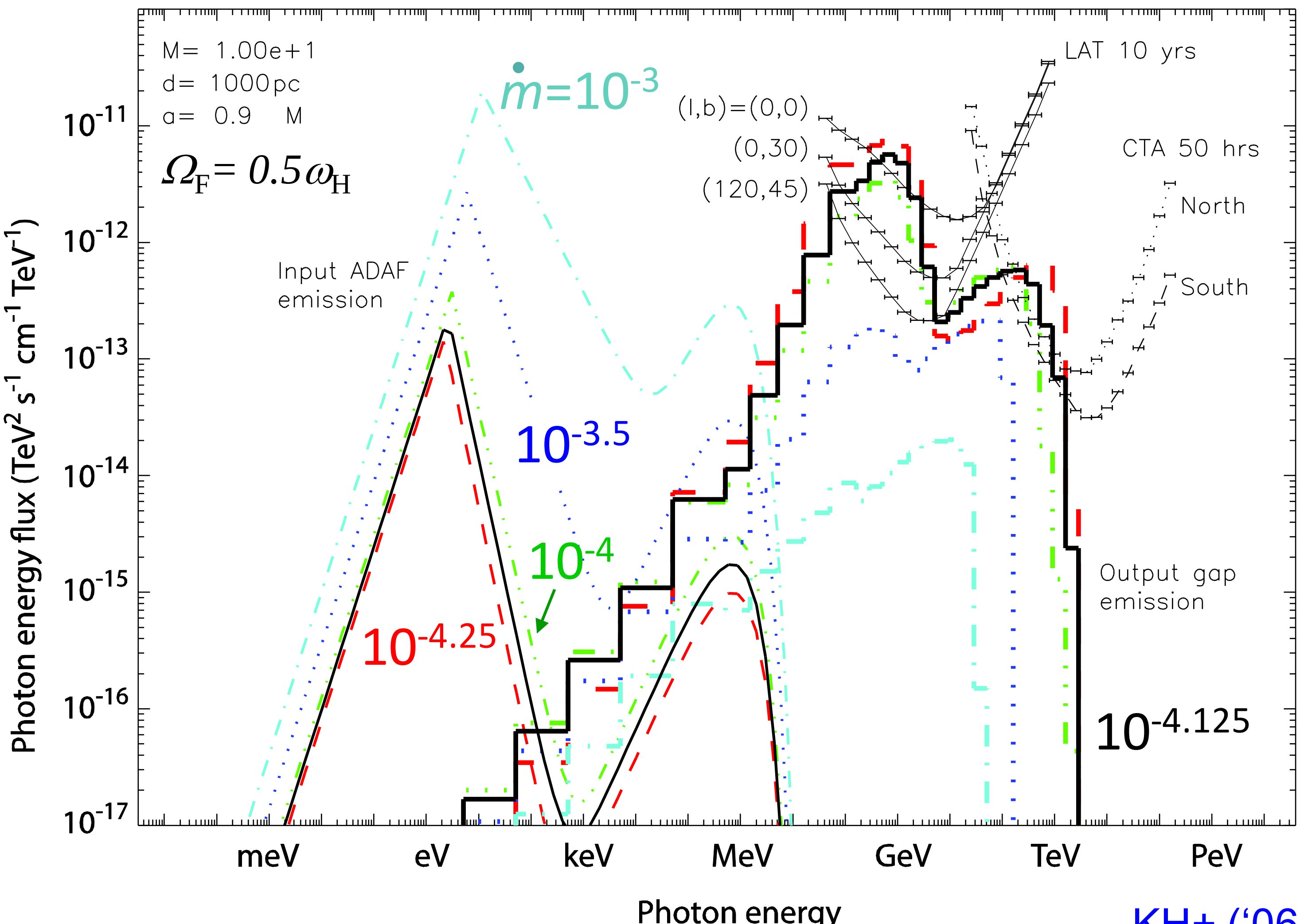

KH+ ('06, ApJ in press)

§ 3 Results: stellar-mass BHs

M=10$M_\odot$, B=B_{eq}; SEDs @ five discrete $\dot{m}$ (θ=0°)

HE flux is detectable if
d<several kpc and
$5.7\times10^{-5} < \dot{M}/\dot{M}_{\rm Edd} < 10^{-4}$

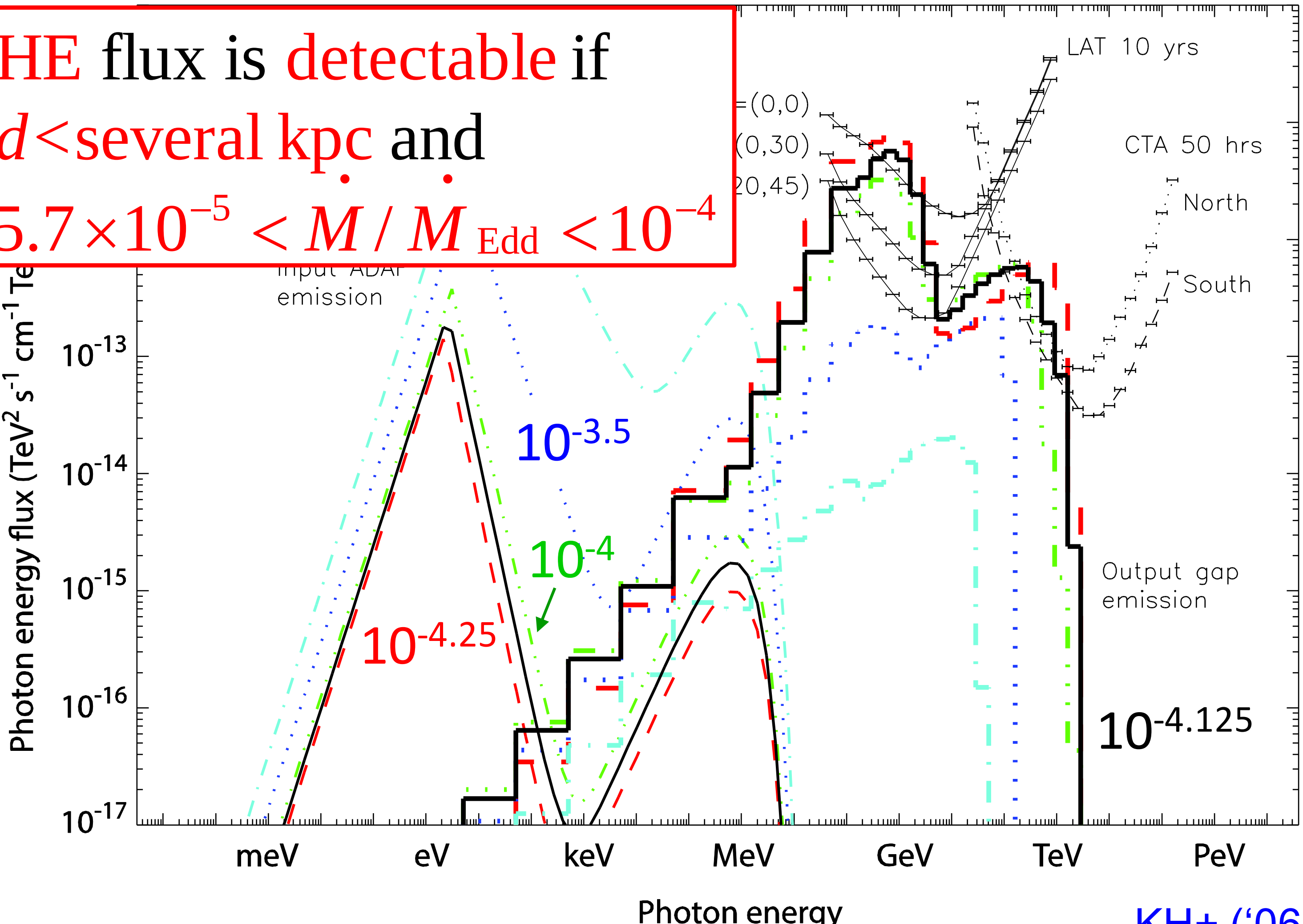

KH+ ('06, ApJ in press)

§ 3 Results: stellar-mass BHs

$M=10M_{\odot}$, $B=B_{eq}$; Emission components ($\theta=0^o$)

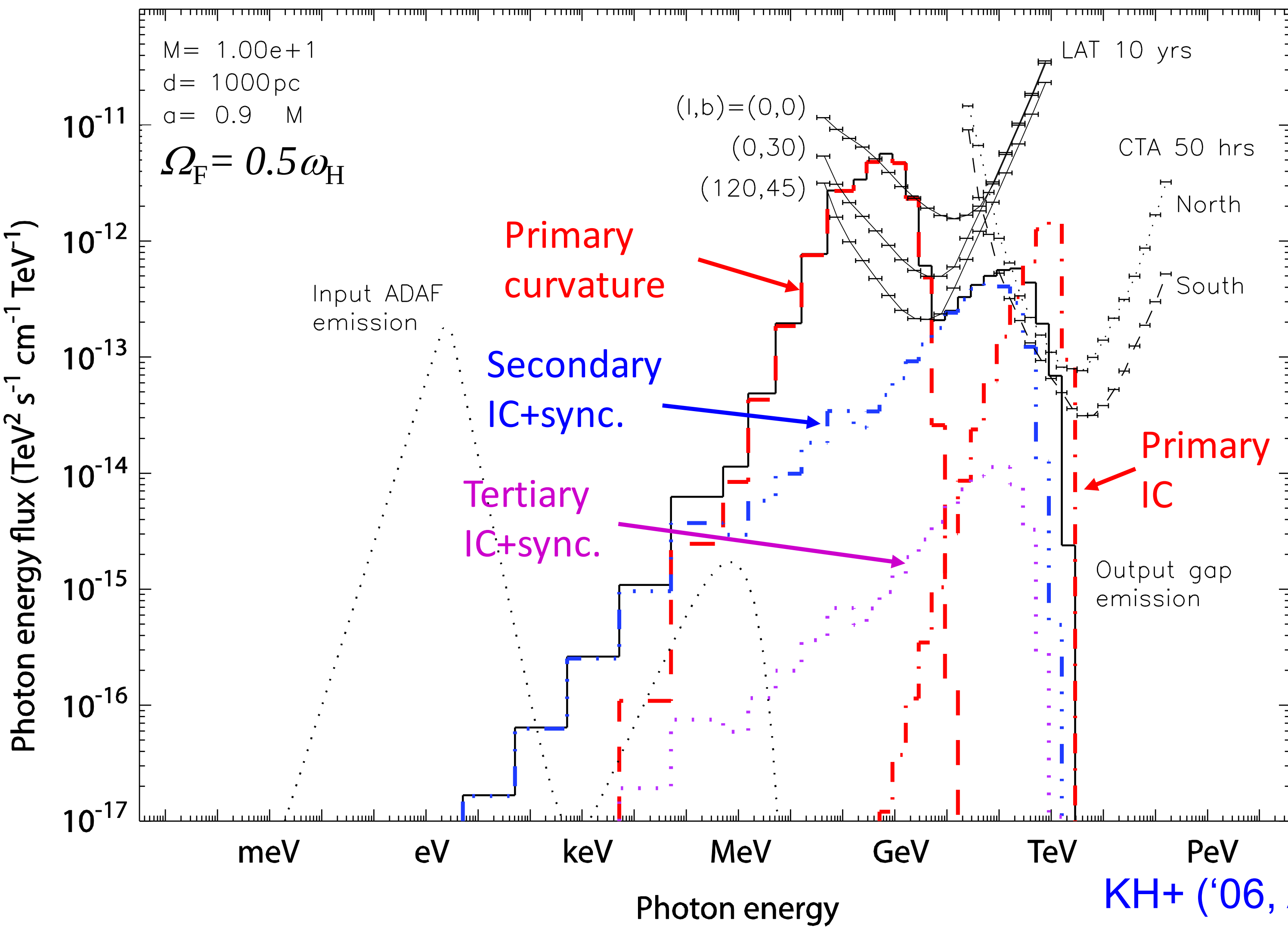

KH+ ('06, ApJ in press)

§ 4 Detectability of BH transients

We can approximately estimate $L_{\rm gap}$ by the Blandford-Znajek flux, $F_{\rm BZ}=L_{\rm BZ}/4\pi d^2$ at Earth.

Four greatest $F_{\rm BZ}$ BHTs (descending order):

Name	mass $M_\odot$	distance kpc	obs. $\dot{M}$ / $\dot{M}_{\rm Edd}$	Comments*
1A 0620-00	6.60	1.06	2.08×10^{-3}	L, T, V616 Mon
4U 1956+350	14.81	1.86		H, P, Cyg X-1
XTE J1118+480	7.30	1.72	4.96×10^{-4}	L, T, KV UMa
GS 2023+338	7.15	2.39	.017-.224	L, T, V404 Cyg

* Low-mass/High-mass companion, Transient/Persistent

We exclude Cyg X-1, because $\dot{M} \gg 10^{-4}\,\dot{M}_{\rm Edd}$.

§ 4 Detectability of BH transients

Although the observed $\dot{M}$ exceeds 10^{-4} for all the 3 BHTs, there may be a certain fraction of time in which

$5.7\times10^{-5} < \dot{M}/\dot{M}_{\rm Edd} < 10^{-4}$ is satisfied.

Name	mass $M_\odot$	distance kpc	obs. $\dot{M}$ / $\dot{M}_{\rm Edd}$	Comments*
1A 0620-00	6.60	1.06	2.08×10^{-3}	L, T, V616 Mon
4U 1956+350	14.81	1.86		H, P, Cyg X-1
XTE J1118+480	7.30	1.72	4.96×10^{-4}	L, T, KV UMa
GS 2023+338	7.15	2.39	.017-.224	L, T, V404 Cyg

* Low-mass/High-mass companion, Transient/Persistent

We thus examine these three BH LMXBs w/ greatest $F_{\rm BZ}$.

§ 4 Detectability of BH transients

J0620-0020: LAT 7-yr averaged flux appears below the theoretical prediction.

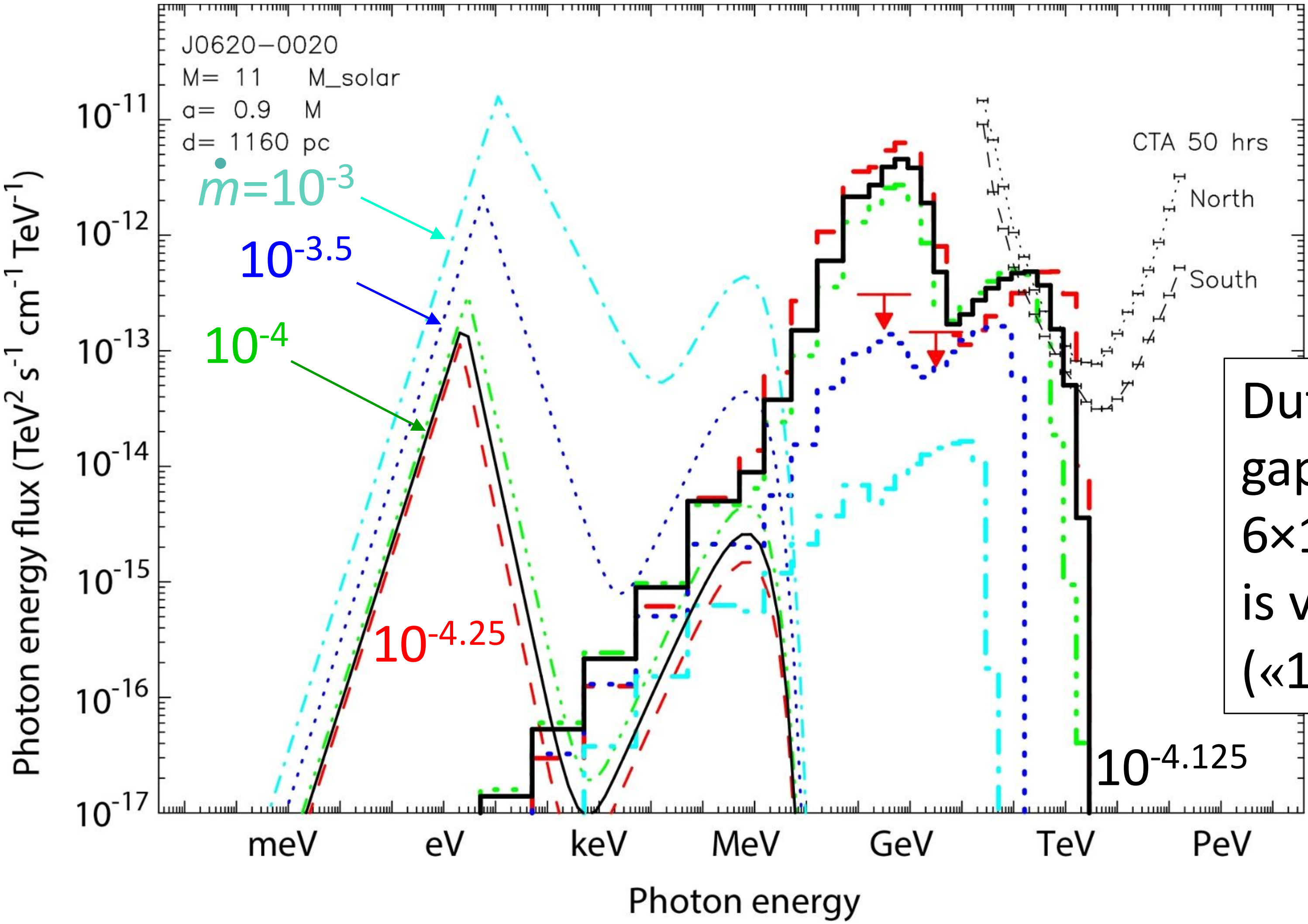

Obs. acc. rate (1917-1975): $\dot{m}\sim 0.002$.

Duty cycle of gap activation $6\times10^{-5}<\dot{m}<10^{-4}$ is very small («1).

Lin + ('16), in prep.

§ 4 Detectability of BH transients

J1118+4802: LAT 7-yr averaged flux also appears below prediction.

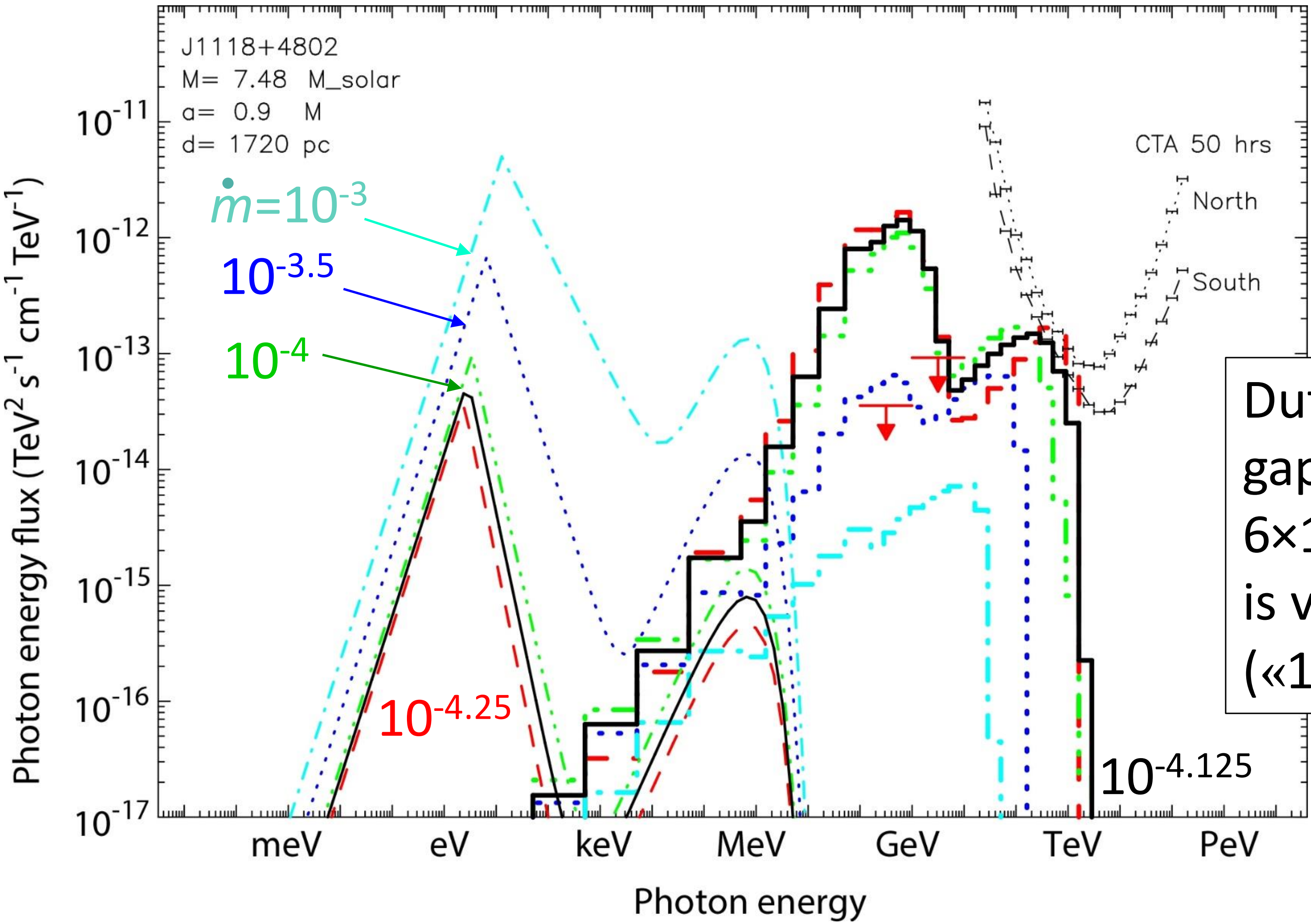

Obs. acc. rate (1998-2015): $\dot{m} \sim 5\times10^{-4}$.

Duty cycle of gap activation $6\times10^{-5}<\dot{m}<10^{-4}$ is very small («1).

Lin + ('16), in prep.

§ 4 Detectability of BH transients

V404 Cyg: LAT 7-yr averaged flux appear slightly below prediction.

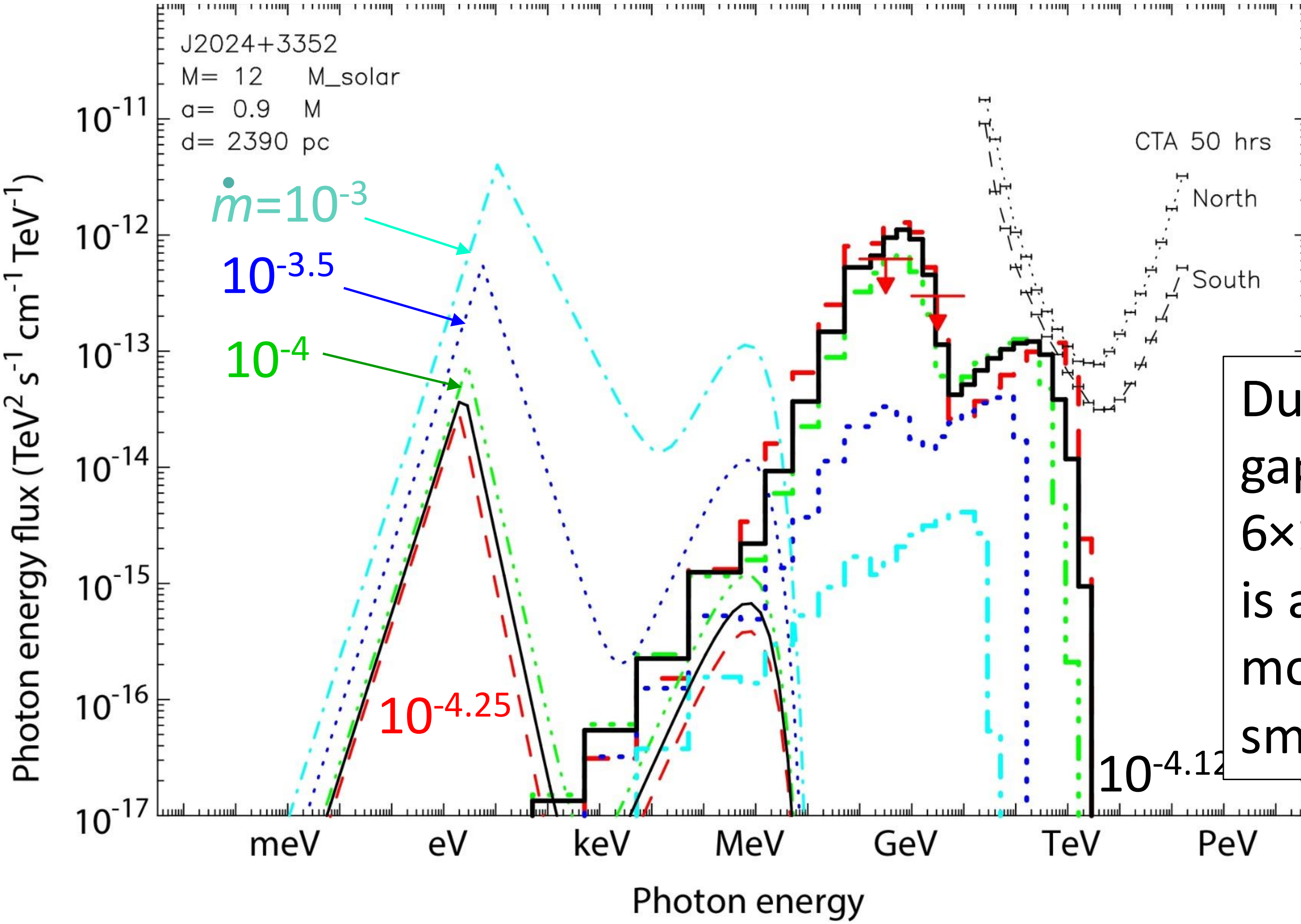

Obs. acc. rate (1995-2005): $\dot{m} > 0.02$.

Duty cycle of gap activation $6\times10^{-5} < \dot{m} < 10^{-4}$ is at least moderately small (<1).

Lin + ('16), in prep.

Summary on BH gap model

- BH gap emits copious HE/VHE γ-rays, if mass accretion resides rate is $10^{-4} > \dot{M}/\dot{M}_{\rm Edd} > 5.7\times10^{-5}$ near the horizon.
- For stellar-mass BHs, $e^{\pm}$'s are accelerated in the gap and saturate @ $\gamma\sim10^7$ by curvature-radiation drag forces.
- For stellar-mass BHs, curvature photons appear at ~GeV and are detectable w/ *Fermi*/LAT, and IC photons appear at 3-30 TeV and are detectable w/ CTA, both during quiescent.
- We can discriminate gap vs. jet emissions by anti-correlation vs. correlations at IR/opt & HE/VHE. Thus, we propose to observe BHTs, J0620-0020, GRO J1655-40, V404 Cyg, J1118+4802, at IR/opt & VHE simultaneously.
- The same method can be applied to arbitrary BH masses, e.g., IMBHs and SMBHs.